A Combined Extended State Observer-Kalman Filter Approach to Robust Greenhouse Climate Control

Hatem SLIMENE[1]*, Houda MATHLOUTHI[2], Chemseddine MAATKI[3], Salim HADJ SAID[4], Walid HASSEN[5], Bilel HADRICH[6], Badr M. ALSHAMMARI[7], Lioua KOLSI[8]

[1] Department of Mechanical Engineering, Higher Institute of Technological Studies of Ksar Hellal, 58 BP Hadj Ali Soua Avenue, Ksar Hellal, 5070, Tunisia
slimene_hatem@yahoo.fr (**Corresponding author*)

[2] Higher Institute of Applied Sciences and Technology, University of Sousse, Taffala City (Ibn Khaldoun), Sousse, 4003, Tunisia
houda.mathlouthi@issatso.u-sousse.tn

[3] Department of Mechanical Engineering, College of Engineering, Imam Mohammad Ibn Saud Islamic University (IMSIU), Riyadh, 11432, Saudi Arabia
casmaatki@imamu.edu.sa

[4] Laboratory of Automation, Electrical Systems and Environment, National Engineering School of Monastir, University of Monastir, Monastir, 5019, Tunisia
salim.hadjsaid@ipeim.rnu.tn

[5] Laboratory of Metrology and Energy Systems, National Engineering School of Monastir, University of Monastir, Monastir, 5019, Tunisia
hassen.walid@gmail.com

[6] Department of Chemical Engineering, College of Engineering, Imam Mohammad Ibn Saud Islamic University (IMSIU), Riyadh, 11432, Saudi Arabia
bmhadrich@imamu.edu.sa

[7] Department of Electrical Engineering, College of Engineering, University of Ha'il, Ha'il, 81451, Saudi Arabia
bms.alshammari@uoh.edu.sa

[8] Department of Mechanical Engineering, College of Engineering, University of Ha'il, Ha'il, 81451, Saudi Arabia
l.kolsi@uoh.edu.sa

Abstract: The precise regulation of temperature and humidity in greenhouses poses a significant control challenge due to the complex, non-linear interactions within the greenhouse climate system, which are further complicated by uncertainties, external influences, and sensor imprecision. This paper introduces a new approach for tackling this challenge, based on the integration of a Kalman filter (KF) and an Extended State Observer (ESO). The ESO is employed for estimating both the unmeasured system variables and the cumulative effect of disturbances. In order to overcome the ESO's sensitivity to measurement noise, a KF is first implemented for filtering the temperature and humidity variables recorded inside the greenhouse. The interconnection between the KF and the ESO is a coupling which is commonly used in advanced automation systems, such as robotics or drone control. This approach enables control and observation algorithms to adapt in real time to variations in the environment, ensuring a robust performance in the face of uncertainties and disturbances. The estimated state and disturbance variables were then integrated into a robust controller based on state feedback linearization and feedforward disturbance compensation. The simulation results confirm the effectiveness of the proposed control strategy for an accurate greenhouse climate management.

Keywords: Disturbance compensation, Extended State Observer, Greenhouse, Kalman Filter, Measurement noise, Robust control.

1. Introduction

Maintaining stable climate conditions within greenhouses is a complex control problem. Although essential for promoting plant growth, these systems, enclosed by transparent materials, exhibit a highly dynamic and nonlinear behaviour and are subject to significant external disturbances such as solar radiation, wind, and fluctuations in temperature and humidity. With the aim of creating an environment conducive to rapid crop development while minimizing the economic impact of production (in terms of resources and energy inputs), various control engineering solutions have been implemented (Chen et al., 2025; Zhang et al., 2020).

Among the advanced control strategies, Wang et al. (2024) present an enhanced nonlinear model predictive control (NMPC) strategy designed to balance greenhouse climate precision with energy efficiency under low-temperature conditions. By combining a wavelet neural network model with an optimized objective function, their approach achieved an energy reduction above 20%, demonstrating its potential for sustainable and energy-efficient greenhouse control. However, it faces challenges related to model complexity and sensitivity to non-measurable disturbances. Zhang et al. (2025) introduce an extended disturbance observer–based sliding mode control (EDO-SMC)

https://doi.org/10.24846/v34i4y202508

approach for four-wheel self-steering (4WSS) agricultural robots, aiming to achieve precise path tracking on irregular and slippery terrains. Through the integration of slip disturbance estimation and adaptive compensation, the proposed method demonstrates an excellent tracking accuracy and robustness, validated by simulation and field test results. However, it is affected by the undesirable phenomenon of chattering (high-frequency oscillations around the sliding surface), which can excite unmodeled dynamics and lead to system instability. Bouketir et al. (2025) present a fuzzy logic-based system designed to optimize greenhouse conditions for tomato cultivation in Algeria by regulating air and soil humidity, temperature, light, and irrigation. Simulation results indicate that this system efficiently automates ventilation, lighting, and irrigation, promoting healthy plant growth and enhancing the crop yield. However, this method relies on an empirical design, significant human expertise, and the careful management of uncertainties in relation to rules and measurements. Escamilla-García et al. (2020) integrated artificial neural networks into greenhouse technologies, thereby contributing to the development of smart agriculture (Industry 4.0).

These technologies enhance the adaptability and accuracy of intelligent control systems responsible for managing the climate and environmental conditions within greenhouses. Thanks to these systems, it is possible to precisely adjust parameters such as temperature and humidity according to environmental variations, thereby making greenhouse management more efficient. However, these approaches require large volumes of reliable data as well as a complex implementation.

Disturbances and uncertainties are inevitable in industrial control systems, making their effective management crucial for maintaining their performance and stability. Chen et al. (2016) present a comprehensive framework for the control of nonlinear systems affected by external disturbances, employing nonlinear Disturbance Observer-Based Control (DOBC) techniques for enhancing system robustness and performance. Within this context, the developed observer enables the estimation of disturbances generated by an exogenous system, whilst ensuring global exponential stability under certain conditions. Qi et al. (2021) and Xiong et al. (2015) developed an Extended State Observer (ESO), useful in model-free control for estimating unknown dynamics. Madonski & Herman (2015) introduced the Active Disturbance Rejection Control (ADRC) architecture, which uses the Extended State Observer (ESO) to provide an accurate real-time estimation of system disturbances. And although the ESO offers advantages in estimating disturbances and unmeasurable state variables (Xue & Huang, 2015; Xue & Huang, 2018), its performance depends on high observer gains, which increase the sensitivity to measurement noise (Lakomy & Madonski, 2021; Shao & Gao, 2016). A hybrid Extended State Observer-Kalman Filter (ESO-KF) approach has recently been developed to overcome these limitations, where the Kalman Filter serves as a pre-filtering stage for enhancing noise suppression and improving disturbance rejection (Bai et al., 2018).

This paper proposes an innovative approach to climate control in agricultural greenhouses by developing a robust system that integrates feedback linearization based on an Extended State Observer (ESO) combined with a Kalman Filter for measurement preprocessing, along with proactive disturbance compensation. Unlike previous studies, which primarily focus on industrial systems or strictly controlled environments, this paper adapts these advanced techniques to the specific challenges of agricultural greenhouses. These challenges include nonlinear disturbances, such as sudden changes in temperature, humidity and solar radiation, that complicate control processes and require a dynamic adaptation, as well as sensor limitations caused by harsh environmental conditions (dust, corrosion), necessitating particularly robust state estimation methods. This innovation effectively addresses the unique demands of greenhouse agriculture, ensuring a precise and reliable climate regulation.

The remainder of this paper is structured as follows. A comprehensive dynamic modelling of the greenhouse climate system is detailed in Section 2, and a feedback linearisation approach for decoupling its non-linear dynamics is presented in Section 3. Further on, Section 4 sets forth the design of a robust controller incorporating an extended state observer (ESO), a Kalman Filter (KF) for state estimation and feedforward disturbance compensation, while Section 5 validates this approach through simulations and the comparison with a Proportional-Integral Sliding Mode control (PISMC) scheme. Finally, Section 6 presents the conclusions of this paper and it outlines the prospects for future research.

2. Greenhouse Dynamic Model

The greenhouse climate model was developed for predicting environmental variables as a function of external inputs (such as solar radiation and ambient temperature), control actions (heating, cooling, ventilation) and the current state of the system. The model is based on a set of differential equations that describe the key phenomena governing the system, including heat transfer by conduction, convection and evaporation, as well as air exchange related to ventilation.

Given the complexity and non-linearity inherent to these phenomena, the proposed model incorporates a specific non-linear dynamics as well as the presence of multiple global disturbances, including sudden variations in the external climatic conditions. To better reflect these complex interactions, the differential equations were reformulated and fitted using experimental data and energy balances, providing a more realistic and robust representation of the greenhouse's climatic behaviour, which is essential for designing effective and reliable control strategies. These differential equations are given as follows (Luan et al., 2012):

$$\begin{aligned}\frac{dT_{in}(t)}{dt} &= \frac{1}{\rho C_P V}\left(Q_{heat}(t) + S_i(t) - \lambda Q_{fog}(t)\right) \\ &\quad - \frac{V_R(t)}{V}(T_{in}(t) - T_{out}(t)) \\ &\quad - \frac{U_A}{\rho C_P V}(T_{in}(t) - T_{out}(t)) \\ &\quad + f_1(T_{in}(t), w_{in}(t), d(t), t)\end{aligned} \tag{1}$$

$$\begin{aligned}\frac{dw_{in}(t)}{dt} &= \frac{1}{\rho V}Q_{fog}(t) + \frac{1}{\rho V}E(S_i(t), w_{in}(t)) \\ &\quad - \frac{V_R(t)}{\rho V}(w_{in}(t) - w_{out}(t)) \\ &\quad + f_2(T_{in}(t), w_{in}(t), d(t), t)\end{aligned} \tag{2}$$

where T_{in} and T_{out} represent the greenhouse's internal and external temperatures (°C), respectively, ρ is the air density (kg/m³), C_p is the specific heat of the air (J/(kg·K)), V is the typical volume of the greenhouse (m³), λ is the latent heat of vaporization (kJ/kg), U_A is the overall heat transfer coefficient (W/(m²·K)), V_R is the ventilation rate (m³/s) and Q_{heat} is the supplemental heat applied to the greenhouse environment (W). S_i is the intercepted solar radiation energy (W/m²), w_{in} and w_{out} represent the internal and external humidity (gH₂O/m³), respectively, Q_{fog} is the water capacity of the fog system (gH₂O/s). The uncertain functions $f_1(T_{in}(t), w_{in}(t), d(t), t)$ and $f_2(T_{in}(t), w_{in}(t), d(t), t)$ include unmodelled dynamics, parameter variations and a complex non-linear behaviour. Furthermore, the final term in the set of variables represents the evapotranspiration function $E(S_i, w_{in})$.

As a preliminary simplification, the evapotranspiration rate $E(S_i, w_{in})$ is approximated as being primarily governed by the intercepted solar radiant energy. This relationship is expressed by the following simplified equation (Gurban et al., 2014):

$$E(S_i(t), w_{in}(t)) = \frac{\alpha}{\lambda}S_i(t) - \beta w_{in}(t) \tag{3}$$

The coefficients α and β account for the influences of several different factors on E from several different factors. As it corresponds to the shading and leaf area, α aggregates those effects on evapotranspiration. The parameter β accounts for various thermodynamics factors. Greenhouses play an important role in managing the temperature and humidity for crops, improving the crop growth conditions, and preserving agricultural products. Evaporative cooling systems can be used effectively, especially in arid regions, where the influence of the incoming relative humidity is relatively small. As a result, the term βw_{in} in equation (3) is relatively small and Q_{heat} in equation (1) is set at zero. The following parameters are defined: $C_0 = (\rho C_p V)$, $V_0 = \rho V$, and $\alpha_0 = \alpha(\lambda \rho V)^{-1}$. Integrating the previous observations, equations (1) and (2) can be expressed as follows:

$$\begin{aligned}\frac{dT_{in}(t)}{dt} &= \frac{1}{C_0}\left(S_i(t) - \lambda Q_{fog}(t)\right) \\ &\quad - \frac{V_R(t)}{V}(T_{in}(t) - T_{out}(t)) \\ &\quad - \frac{U_A}{C_0}(T_{in}(t) - T_{out}(t)) \\ &\quad + f_1(T_{in}(t), w_{in}(t), d(t), t)\end{aligned} \tag{4}$$

$$\begin{aligned}\frac{dw_{in}(t)}{dt} &= \frac{1}{V_0}Q_{fog}(t) + \alpha_0 S_i(t) \\ &\quad - \frac{V_R(t)}{V_0}(w_{in}(t) - w_{out}(t)) \\ &\quad + f_2(T_{in}(t), w_{in}(t), d(t), t).\end{aligned} \tag{5}$$

3. Feedback Linearization Control

The first step of the robust control strategy is to apply a linearized control law to agricultural greenhouses. This enables the effective management of the complex nonlinear dynamics of the indoor climate, improves control accuracy and stability, and enables a better disturbance handling and an optimal decoupling of key variables (Wu et al., 2024). The greenhouse model can then be reformulated as a nonlinear MIMO system, suitable for designing a feedback linearization controller (Sun et al., 2021):

$$\begin{cases} \dot{x} = Ax + B_u(x,v)u + Dv + B_d f(x,d(t),t) \\ y = C_m x + y_{noise} \end{cases} \quad (6)$$

with:

$$A = \begin{bmatrix} -\frac{U_A}{C_0} & 0 \\ 0 & 0 \end{bmatrix},\ B_u(x,v) = \begin{bmatrix} -\frac{1}{V}(x_1 - v_2) & -\frac{\lambda}{C_0} \\ -\frac{1}{V_0}(x_2 - v_3) & \frac{1}{V_0} \end{bmatrix},$$

$$D = \begin{bmatrix} \frac{1}{C_0} & \frac{U_A}{C_0} & 0 \\ \alpha_0 & 0 & 0 \end{bmatrix},\ B_d = \begin{bmatrix} b_1 \\ b_2 \end{bmatrix},\ C_m = \begin{bmatrix} 1 & 0 \\ 0 & 1 \end{bmatrix},$$

where:

$x = [T_{in}, w_{in}]^T$ is the state variable;

$u = [V_R, Q_{fog}]^T$ is the control variable;

$v = [S_i, T_{out}, w_{out}]^T$ is the measured outside disturbance variable;

$y = [T_{inS}, w_{inS}]^T$ is the system output;

$y_{noise} = [y_{noiseT}, y_{noisew}]^T$ is the noise for temperature and humidity;

$f(x,d(t),t)$ represents the global uncertain function, encompassing the unmodelled internal dynamics dependent on the state x, as well as the unmeasured disturbances denoted by $d(t)$.

These components are modelled by the functions f_1 and f_2, respectively. To simplify the controller synthesis, a proportional relationship is assumed between these functions:

$f_1 = b_1 f$, and $f_2 = b_2 f$,

where b_1 and b_2 are proportionality coefficients (constant or variable), determined according to the assumptions of the dynamic model.

The control matrix $B_u(x,v)$, although nonlinear, is invertible at each computation step under specific conditions, notably when the matrix is full rank (i.e. its determinant is nonzero), the variables x and v belong to a domain where the coefficients of B_u remain bounded and continuous, and the system does not exhibit singularities or discontinuities within the considered interval.

Based on the previous condition and considering a reference trajectory r, defined by the setpoint variables r_T and r_w, the application of the feedback linearization method leads to the following expression (Chen et al., 2018):

$$\dot{x} = r \quad (7)$$

where $r = [r_T, r_w]^T$ is the new input vector in the transformed coordinate system.

Based on equations (6) and (7), the feedback linearization control (FLC) law is designed as follows (Gao et al., 2014):

$$u_{FB} = B_u^{-1}(r - Ax - Dv - B_d f(x,d(t),t)). \quad (8)$$

4. Robust Control Strategy

The robust control strategy for agricultural greenhouses is structured around four main steps: first, the design of the extended model of the greenhouse, second, the development of a combined ESO-KF structure, third, an in-depth analysis of the robust control law, and finally, the determination of the Kalman Filter gain using the Riccati equation.

4.1 Extended Greenhouse Model

ESO is a key tool for estimating, in real time, the system state variables that are not directly measurable, such as temperature and humidity inside the greenhouse. It is also used for detecting and compensating for external disturbances (climatic variations, unexpected inputs of humidity or heat) that may affect the system. This accurate estimation of system states and disturbances is essential for ensuring a reliable control despite the uncertainties and variations in the dynamic model of the greenhouse.

In ESO-based control, the global disturbance d_e is modelled as an extended system variable, that is exogenous, and independent of the dynamics of the internal state of the system (Li et al., 2012):

$$x_3 = d_e = f(x,d(t),t), \quad (9)$$

which should be added to the system in equation (6). The extended system is then rewritten as follows:

$$\begin{cases} \dot{\bar{x}} = \bar{A}\bar{x} + \bar{B}_u u + \bar{D}v + Fh(t) \\ y = \bar{C}_m \bar{x} + y_{noise} \end{cases} \quad (10)$$

where the extended state variable $\bar{x} = \left[x^T, d_e\right]^T$, and $h(t) = \dot{x}_3 = \dot{d}_e$ with:

$$\bar{A} = \begin{bmatrix} -\frac{U_A}{C_0} & 0 & b_1 \\ 0 & 0 & b_2 \\ 0 & 0 & 0 \end{bmatrix}, \; \bar{B}_u = \begin{bmatrix} -\frac{1}{V}(x_1 - v_2) & -\frac{\lambda}{C_0} \\ -\frac{1}{V_0}(x_2 - v_3) & \frac{1}{V_0} \\ 0 & 0 \end{bmatrix},$$

$$\bar{D} = \begin{bmatrix} \frac{1}{C_0} & \frac{U_A}{C_0} & 0 \\ \alpha_0 & 0 & 0 \\ 0 & 0 & 0 \end{bmatrix}, F = \begin{bmatrix} 0 \\ 0 \\ 1 \end{bmatrix}, \; \bar{C}_m = \begin{bmatrix} 1 & 0 & 0 \\ 0 & 1 & 0 \end{bmatrix}.$$

4.2 Combined ESO-Kalman Filter Structure

To further improve the quality of the estimates, the ESO is combined with a KF. The latter is an optimal filtering algorithm that refines the estimates by considering noisy measurements and statistical uncertainties. This hybrid ESO-KF approach is more robust to non-stationary disturbances and measurement errors, guaranteeing a more stable and reliable estimation of the system states and external disturbances.

The equation governing the Kalman Filter is expressed as follows (Bai et al., 2018):

$$\dot{\hat{x}} = A\hat{x} + B_u u + Dv + B_d d_e + K_f (y - C_m \hat{x}) \quad (11)$$

where $\hat{x}$ represents the a posteriori estimate of x (i.e. after correction) obtained using the KF, and K_f is the gain matrix of the steady-state Kalman filter.

The ESO model can represent both the dynamics of the system and the evolution of disturbances, making it easier to estimate them in real time:

$$\dot{z} = \bar{A}z + \bar{B}_u u + \bar{D}v + K_e (y - \bar{C}_m z) \quad (12)$$

where $z = [z_x^T, \hat{d}_e]^T$ is the estimate of $\bar{x}$, z_x is the estimate of x, and $z_3 = \hat{d}_e$ is the estimate of the overall disturbance, all these variables being obtained through the ESO, and K_e denotes the gain matrix of the ESO.

By replacing the lumped perturbation d_e related to the KF (equation (11)) with the estimate $\hat{d}_e$, and the actual output signal y in ESO (equation (12) with the estimate $C_m\hat{x}$, the resulting continuously updated ESO-KF interconnected structure can be expressed as follows:

$$\begin{cases} \dot{\hat{x}} = A\hat{x} + B_u u + Dv + B_d \hat{d}_e + K_f (y - C_m \hat{x}) \\ \dot{z} = \bar{A}z + \bar{B}_u u + \bar{D}v + K_e (C_m \hat{x} - \bar{C}_m z) \end{cases} \quad (13)$$

4.3 Robust Control Law Expression

The implementation of a robust controller based on the use of estimated system state variables and the estimation of external disturbances proves essential in order to compensate for the inaccuracies inherent to direct measurements, the frequent unavailability of sensors under severe climatic conditions, as well as sensor failures or their gradual degradation. By integrating advanced observers such as the Extended State Observer combined with the Kalman Filter, this type of regulator provides a reliable, real-time estimation of the critical variables and disturbances, thus ensuring a precise and stable control despite model uncertainties and challenging operational conditions. This approach significantly enhances the robustness of the control system by guaranteeing the continuity and quality of greenhouse microclimate regulation while reducing its dependence on often noisy or missing direct measurements (Bennis et al. 2008).

The robust command is formulated as the sum of two components:

- u_{FB}, denoting feedback control, which corrects in real time any differences between the estimated states, represented by z_x and the setpoint values, ensuring stability and accuracy;
- u_{FF}, denoting feedforward control, which acts in anticipation of the estimated disturbances $\hat{d}_e$, improving responsiveness and compensation for external effects.

This allows to express the robust control law in a comprehensive form:

$$\begin{aligned} u &= u_{FB}(z_x) + u_{FF}(\hat{d}_e) \\ &= u_{FB}(z_x) + K_d \hat{d}_e. \end{aligned} \quad (14)$$

where K_d is the disturbance compensation gain.

In the context of this hybrid structure, the feedback control law is defined as follows:

$$u_{FB}(z_x) = B_u^{-1}(r - Az_x - Dv - B_d d_e) \quad (15)$$

The adjustment of the gains in the ESO-KF hybrid structure, and also of the K_d gain of the u_{FF} is decisive in optimizing the compromise between convergence speed, stability and robustness to disturbances.

4.4 KF Gain Determination

Assumption: the noise expressed by $y_{noise}(t)$ and the unmeasurable disturbances denoted by $d_e(t)$ are:

- stationary, meaning their statistical properties (mean, variance) remain constant over time or,
- independent, indicating that there is no correlation between the two noises.

Consequently, the corresponding covariances are expressed as follows (Schneider & Georgakis, 2013):

$$\begin{aligned} E\left\{d_e(t)d_e(t+\tau)^T\right\} &= Q\delta(\tau), \\ E\left\{y_{noise}(t)y_{noise}(t+\tau)^T\right\} &= R\delta(\tau), \\ E\left\{y_{noise}(t)d_e(t+\tau)^T\right\} &= 0, \end{aligned} \tag{16}$$

where Q is the disturbance estimation covariance, R is the measurement noise covariance, and δ is the unit pulse function.

The Kalman gain K_f is determined for minimizing the variance of the estimation error $\varepsilon_x = x - \hat{x}$ of the steady state system.

It should be noted that $P_f = E\left\{\varepsilon_x \varepsilon_x^T\right\}$ is the covariance matrix of the estimation error (of dimension 2×2) satisfying the following differential equation (Nicholas & Maria, 2013):

$$\dot{P}_f = AP_f + P_f A^T - P_f C_m^T R^{-1} C_m P_f + B_d Q B_d^T. \tag{17}$$

The Kalman gain formula is given by:

$$K_f = P_f C_m^T R^{-1}. \tag{18}$$

Remark: The input-to-state stability (ISS) of the system in equation (6), under the robust control law in equation (14), is guaranteed if the disturbances d_e and the noises y_{noise} are bounded, and if the gains K_f of the KF filter in steady state, K_e of the state observer as expressed in equation (13), and K_d related to the feedback control law as expressed in equation (14) are chosen such that the matrix A_0 is a Hurwitz matrix. This condition ensures stability despite the uncertainties and variations in measurements (a sketch of the stability proof is given in Appendix A).

5. Simulation Results

The proposed robust control strategy was evaluated with regard to its effectiveness and performance using a numerical simulation. A case study was then carried out to demonstrate the effectiveness of the robust control scheme illustrated in Figure 1. The system parameter values are as follows: the value of ρ is approximately 1.2 kg/m³, the value of C_p is about 1006 J/(kg·K), that of V is approximately 57.6 m³, the value of λ is 2256 kJ/kg, and that of U_A is 10.08 J/(m²·K). The model parameters expressed in equations (4) and (5) were set as C_0 = 69.53 kJ/K, V_0 = 69.12 kg, and α_0 = 0.00083.

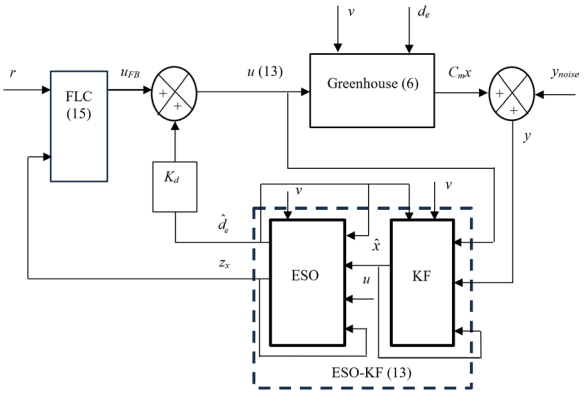

Figure 1. General robust control scheme based on the proposed combination between an Extended State Observer and a Kalman Filter

To validate the performance of the proposed controller, it was compared with the Proportional-Integral Sliding Mode Control approach.

5.1 PI Sliding Mode Control Technique

Lammari et al. (2020) have proposed the Proportional-Integral Sliding Mode Control (PISMC), which is crucial for controlling the indoor environment of greenhouses. This method combines the advantages of PI controllers, which ensure accuracy in following the desired trajectories, with those of SMC, which offer robustness against disturbances and parametric uncertainties. The controller is expressed as follows:

$$\begin{aligned} u &= u_{PI}(t) + u_{SMC}(t) \\ &= k_p e(t) + k_i \int_0^t e(\tau)d\tau - U\ sat(\sigma,\varepsilon), \end{aligned} \tag{19}$$

where $e(t) = r(t) - y(t)$ is the tracking error, k_p is the proportional gain, k_i is the integral gain, U is a positive constant of significant value, $sat(\sigma,\varepsilon) = \dfrac{\sigma}{|\sigma| + \varepsilon}$ is a saturation function, and ε

is a positive design constant used for attenuating chattering, and the switching function can be formulated as $\sigma = e$.

The optimum values for the PISMC controller gains for temperature and humidity are $k_p = 0{,}1285$ and $k_i = 0{,}1285$, with $U = 0.2552$ and $\varepsilon = 0.1$.

5.2 Robust Control Parameters

The parameters of the ESO-KF-based robust control for temperature and humidity were chosen as follows to achieve a good control performance:

The ESO gain matrix is $K_e = \begin{bmatrix} 22.33 & 7.68 \\ 7.31 & 22.76 \\ 97.05 & 102.95 \end{bmatrix}$,

and the KF parameters P_0, R, and Q are chosen as:

$P_0 = \begin{bmatrix} 10 & 0 \\ 0 & 10 \end{bmatrix}$, $R = \begin{bmatrix} 1 & 0 \\ 0 & 1 \end{bmatrix}$, $Q = 100$, and

$K_d = \begin{bmatrix} -0.01 \\ -0.01 \end{bmatrix}$.

where P_0 denotes an initial covariance matrix of the estimation error.

To guarantee both asymptotic stability and the rapid estimation of the system state x and the external disturbance d_e, the gain K_e of the ESO observer must be rigorously optimized.

This gain is determined using the pole placement method applied to the matrix $\bar{A} - K_e \bar{C}_m$. The poles are chosen to be sufficiently close to each other to ensure a consistent dynamics. In this context, the selected desired poles are [-10,-15,-20], ensuring a robust stability and an optimal compromise between the convergence speed and computational simplicity.

5.3 Performances Obtained by Both Controllers

A 320-minute setpoint tracking simulation was conducted to evaluate the performance and effectiveness of the proposed robust control strategy.

The initial conditions inside the greenhouse, regarding temperature and humidity, both for the KF and the ESO, were set at 18 °C and 26 gH_2O/m^3, respectively. The outdoor climatic conditions were modelled by step signals and set as follows: a solar irradiance S_i of 500W/m^2, an outdoor temperature T_{out} of 32°C, and an outdoor humidity w_{out} of 10gH_2O/m^3. The indoor temperature setpoint remained constant at 20 °C for the first 150 minutes before being raised to 25 °C. Simultaneously, the humidity setpoint was adjusted, decreasing from 28 to 22 gH_2O/m^3. Furthermore, the model incorporates unknown and time-varying disturbances expressed by d_e correlated with fluctuations in external weather conditions, in order to accurately reproduce the real variations of temperature and humidity inside the greenhouse.

The indoor temperature and humidity monitoring performance is shown in Figures 2 and 3. After the setpoint change at minute 150 of the setpoint tracking simulation, both controllers reach the new setpoints (25 °C for temperature and 22 gH2O/m^3 for humidity) within less than 10 minutes, demonstrating a fast dynamic response. However, the ESO-KF-based controller enables a significantly more accurate convergence, with an overshoot of less than +0.3 °C for temperature (with the peak at around 25.3 °C) and less than -0.25 gH_2O/m^3 for humidity.

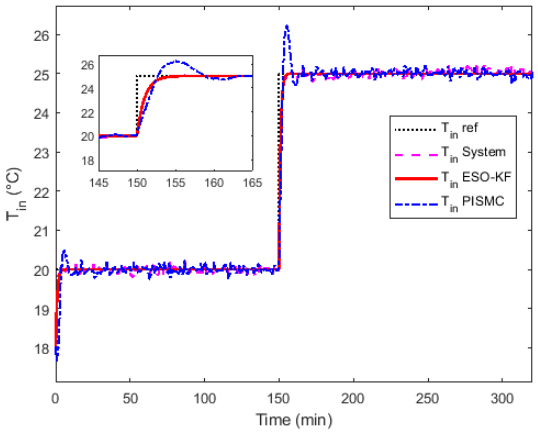

Figure 2. Tracking performances for the greenhouse indoor temperature

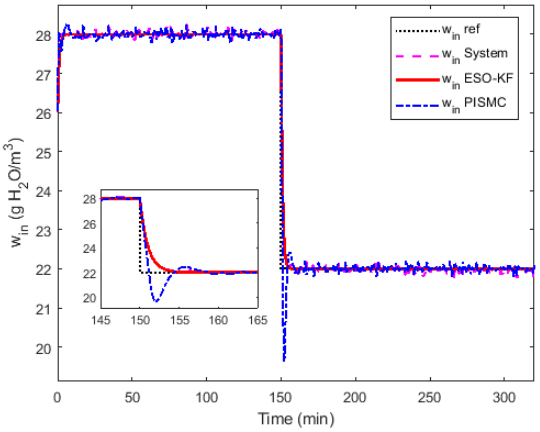

Figure 3. Tracking performances for the greenhouse indoor humidity

On the other hand, the PISMC controller exhibits more pronounced transient variations: a temperature overshoot of approximately +1.2 °C (with the peak at 26.2 °C) and a negative humidity overshoot of up to -2 gH_2O/m^3 (the minimum at 20 gH_2O/m^3 for a setpoint of 22 gH_2O/m^3). Additionally, it shows more significant oscillations around the setpoints, indicating a greater sensitivity to rapid changes and external disturbances. These quantitative results confirm that the robust controller significantly reduces the overshoot and improves disturbance rejection, which make it more suitable for maintaining stable and accurate climate conditions inside the greenhouse in comparison with the PISMC strategy.

Figures 4 and 5 illustrate the greenhouse temperature and humidity monitoring errors, highlighting the superiority of the robust controller. Due to its advanced estimation capabilities, it significantly reduces the deviations from setpoints. Specifically, the errors under the ESO-KF control remain very small and are quickly absorbed after each setpoint change, whereas the PISMC generates larger variations.

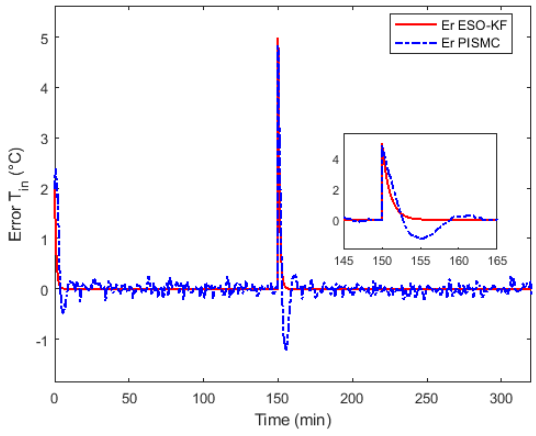

Figure 4. Greenhouse temperature error

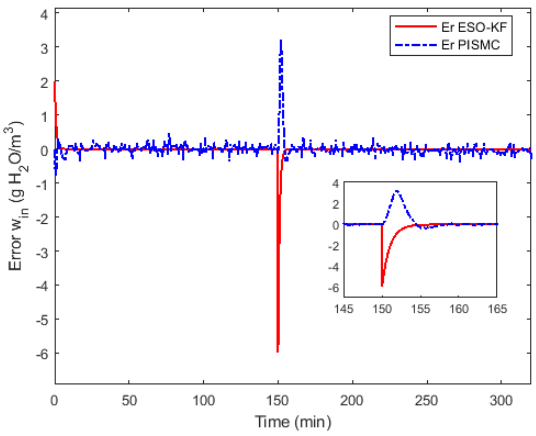

Figure 5. Greenhouse humidity error

Figures 6 and 7 illustrate the control actions of the V_R ventilation and Q_{fog} misting systems. The results show that, under the robust control, the ventilation and humidification rates exhibit a rapid transient dynamics while remaining within acceptable operational limits, the ventilation varies smoothly between 20% and 60% of the capacity, while misting varies between 0 and 30 units (an arbitrary scale) without abrupt peaks. The PISMC controller, on the other hand, generates a more pronounced chattering phenomenon, with ventilation rates fluctuating sharply above 70% and misting levels showing irregular peaks. This chattering can place a significant stress on the actuators, increasing wear and reducing the system`s reliability.

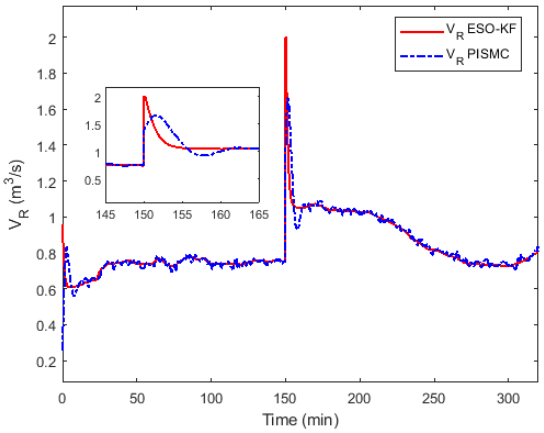

Figure 6. Time evolution for the ventilation rate generated by the employed controllers

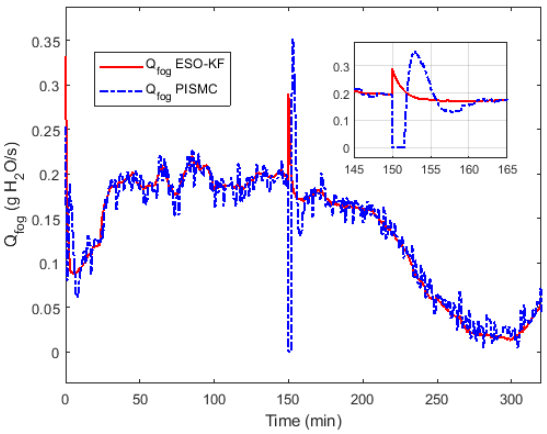

Figure 7. Time evolution for the Q_{fog} rate generated by the employed controllers

As illustrated in Figure 8, the time evolution of the lumped disturbances and their estimated values exhibit good agreement, which demonstrates the performance of the ESO.

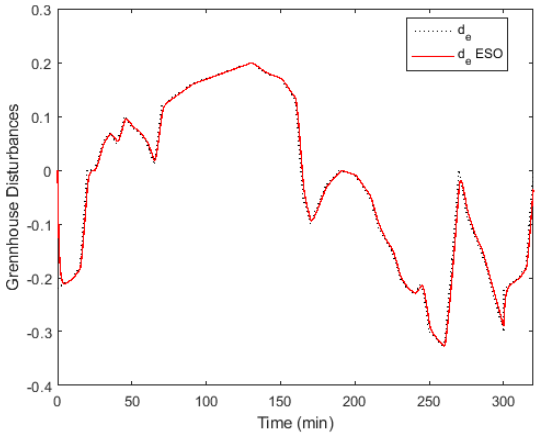

Figure 8. Estimation of greenhouse lumped disturbances

Table 1 compares the performance of the robust controller and PISMC controller using conventional time domain indices. The MSE values show significant differences in terms of accuracy and stability. The robust controller reduces the MSE for temperature by around 50% in comparison with the PISMC, thanks to its real-time estimation and active filtering of disturbances, allowing an optimum compensation for uncertainties and noise. For humidity, although the reduction in MSE is less pronounced (around 11%), the robust controller still retains a significant advantage over the PISMC controller. The lower values for the standard error of the variance obtained with robust control, in comparison with those obtained with the PISMC, indicate the superior performance of the former in terms of control accuracy and reliability. This improvement is crucial for the effective optimization of the climatic conditions inside the greenhouse. Finally, the temperature overshoot obtained based on the robust strategy is limited to 1.1368%, whereas it reaches 4.94% with the PISMC method, a difference almost equal to a factor of four. The difference is even higher for humidity: the robust strategy maintains the overshoot at 0.87%, while the PISMC approach records a much higher peak, reaching 10.45%. This performance demonstrates the ability of the robust controller to limit transient fluctuations, reducing the risk of overheating or thermal instability in the greenhouse.

In the context of climate control in agricultural greenhouses, this analysis shows that the use of a robust regulator offers advantages in terms of sensitivity and ease of use in comparison with a PISMC controller. The former provides a better resistance to variations and disturbances, ensuring a stable performance in the face of frequent fluctuations in climate parameters. Its ability to adapt quickly and accurately improves the sensitivity of the control system, which is essential for maintaining the optimal conditions for plant growth. In addition, the simplicity of its configuration and integration facilitates its deployment, which is not the case for PISMC, which requires an in-depth expertise for adjusting the parameters of the sliding mode. Designed for managing the non-linearities and uncertainties inherent to greenhouses, the robust controller ensures an increased stability and accuracy, optimising climate management while improving crop quality, extending the crop growth period and increasing the crop yield.

Table 1. Results for the tracking performance comparison with regard to the step response

Performance index		Robust controller	PISMC
MSE	T_{in}	0.0667	0.1336
	w_{in}	0.0874	0.0974
Standard error	T_{in}	0.0808	0.0832
of the variance	w_{in}	0.1163	0.1168
Overshoot (%)	T_{in}	1.1368	4.9401
	w_{in}	0.87	10.45

6. Conclusion

Precise climate control in agricultural greenhouses is traditionally disrupted by environmental variations and measurement noise, which degrades the performance of control systems. This study brings about a significant advancement by proposing a high-precision controller combining two complementary mechanisms: a dynamic servo control of thermal setpoints and an active compensation for external disturbances. The main objective of this paper is the implementation of a robust controller based on state feedback linearization coupled with anticipatory disturbance compensation, integrating an Extended State Observer associated with a Kalman filter (ESO-KF). This architecture optimizes the estimation of critical parameters while significantly reducing their dependence on conventional physical sensors for the system`s state. However, it still requires specific sensors for measuring external disturbances such as outside temperature,

ambient humidity and sunlight. Thus, the ESO-KF improves the robustness and accuracy of real-time estimates, even in the presence of noise and uncertainties. The comparative tests which were carried out involving the robust controller and the PISMC have demonstrated that the robust controller offers a significant improvement in robustness against the unmeasured variations, as well as a significant reduction in stabilization times. In addition, it is very easy to apply the proposed controller in real-world scenarios due to an architecture that is less dependent on complex settings. This innovative solution opens new possibilities for agricultural operations, particularly in terms of energy savings and hygrothermal stability. Future research directions could focus on validating this approach on an experimental platform equipped with variable modulation actuators and adaptive supervision interfaces. This validation will make it possible to quantify the operational gains under real production conditions, particularly for crops that are sensitive to micro-climate disturbances.

Acknowledgements

This work was supported and funded by the Deanship of Scientific Research at Imam Mohammad Ibn Saud Islamic University (IMSIU) (Grant no. IMSIU-DDRSP2503).

Appendix A: Sketch of the stability proof

The state error of the system $\varepsilon_x = x - \hat{x}$, and the disturbance error $\varepsilon_{d_e} = d_e - \hat{d}_e$ are considered.

By using equations (6) and (13), the derivative of the state error can be expressed as:

$$\begin{aligned}\dot{\varepsilon}_x &= \dot{x} - \dot{\hat{x}} \\ &= (A - K_f C_m)\varepsilon_x + B_d \varepsilon_{d_e} - K_f y_{noise}\end{aligned} \tag{A1}$$

The state estimate error is expressed as:

$$\varepsilon_z = \overline{x} - z = \begin{bmatrix} x \\ d_e \end{bmatrix} - \begin{bmatrix} z_x \\ \hat{d}_e \end{bmatrix} \tag{A2}$$

Using equations (10) and (13), the derivate of ε_z can be obtained:

$$\begin{aligned}\dot{\varepsilon}_z &= \dot{\overline{x}} - \dot{z} \\ &= (\overline{A} - K_e \overline{C}_m)\varepsilon_z + K_e C_m \varepsilon_x + Fh\end{aligned} \tag{A3}$$

Then, the estimation errors for the ESO-KF controller are expressed as follows:

$$\varepsilon_0 = \begin{bmatrix} \varepsilon_x \\ \varepsilon_z \end{bmatrix} = \begin{bmatrix} x \\ x \\ d_e \end{bmatrix} - \begin{bmatrix} \hat{x} \\ z_x \\ \hat{d}_e \end{bmatrix} \tag{A4}$$

By combining equations (A1) and (A3), the observer error dynamics can be expressed as:

$$\dot{\varepsilon}_0 = A_0 \varepsilon_0 + \dot{d}_e \tag{A5}$$

where:

$$A_0 = \begin{bmatrix} A - K_f C_m & \overline{B}_d \\ K_e C_m & \overline{A} - K_e \overline{C}_m \end{bmatrix},\ \overline{B}_d = \begin{bmatrix} 0_{2\times 2} & B_d \end{bmatrix},$$

and $\dot{d}_e = \begin{bmatrix} -K_f y_{noise} \\ Fh \end{bmatrix}$

The following quadratic Lyapunov function is considered:

$$V(\varepsilon_0) = \varepsilon_0^{\,T} P_0 \varepsilon_0 \tag{A6}$$

Therefore, as A_0 is a Hurwitz matrix, there exists a positive definite matrix P_0 that satisfies a Lyapunov equation:

$$A_0^{\,T} P_0 + P_0 A_0 = -I_{5\times 5}$$

By using the derivative of $V(\varepsilon_o)$ the following is obtained:

$$\begin{aligned}\dot{V}(\varepsilon_0) &= -\varepsilon_0^{\,T}\varepsilon_0 + 2\dot{d}_e^{\,T} P_0 \varepsilon_0 \\ &\le -\|\varepsilon_0\|^2 + 2\sigma_{\max}(P_0)\|\overline{d}_e\|\|\varepsilon_0\| \\ &\le -\|\varepsilon_0\|^2 + \xi\|\varepsilon_0\|^2 - \xi\|\varepsilon_0\|^2 + 2\sigma_{\max}(P_0)\|\overline{d}_e\|\|\varepsilon_0\|\end{aligned} \tag{A7}$$

Finally, the following condition is found:

$$\dot{V}(\varepsilon_0) \le -(1-\xi)\|\varepsilon_0\|^2 - M(\varepsilon_0), \tag{A8}$$

where:

$M(\varepsilon_0) = \left[\xi\|\varepsilon_0\| - 2\sigma_{\max}(P_0)\|\overline{d}_e\|\right]\|\varepsilon_0\|$, and $\xi \prec 1$.
$M(\varepsilon_0) \succ 0$ was obtained. In this regard:

$$\|\varepsilon_0\| \succ \frac{2\sigma_{\max}(P_0)\|\overline{d}_e\|}{\xi} \cong \mu \succ 0 \tag{A9}$$

Consequently, inequality (A8) satisfies:

$$\dot{V}(\varepsilon_0) \le -(1-\xi)\|\varepsilon_0\|^2,\ \forall\|\varepsilon_0\| \ge \mu \succ 0. \tag{A10}$$

REFERENCES

Bai, W., Xue, W., Huang, Y. et al. (2018) On extended state based Kalman filter design for a class of nonlinear time-varying uncertain systems. *Science China Information Sciences.* 61(4), Art. ID. 042201. https://doi.org/10.1007/s11432-017-9242-8.

Bennis, N., Duplaix, J., Enea, G. et al. (2008) Greenhouse climate modelling and robust control. *Computers and Electronics in Agriculture*. 61(2), 96-107. https://doi.org/10.1016/j.compag.2007.09.014.

Bouketir, O., Saib, A., & Fenni, A. (2025) A Fuzzy Logic-Based Greenhouse Smart System for Sustainable Tomato Production in Algeria. *Engineering, Technology & Applied Science Research*. 15(4), 24110-24116. https://doi.org/10.48084/etasr.10856.

Chen, L., Du, S., Xu, D. et al. (2018) Sliding Mode Control Based on Disturbance Observer for Greenhouse Climate Systems. *Mathematical Problems in Engineering*. 2018(3), Art. ID 2071585. https://doi.org/10.1155/2018/2071585.

Chen, S., Liu, A., Tang, F. et al. (2025) A Review of Environmental Control Strategies and Models for Modern Agricultural Greenhouses. *Sensors.* 25(5), Art. ID 1388. https://doi.org/10.3390/s25051388.

Chen, W.-H., Yang, J., Guo, L. et al. (2016) Disturbance-Observer-Based Control and Related Methods - An Overview. *IEEE Transactions on Industrial Electronics*. 63(2), 1083-1095. https://doi.org/10.1109/TIE.2015.2478397.

Escamilla-García, A., Soto-Zarazúa, G. M., Toledano-Ayala, M. et al. (2020) Applications of Artificial Neural Networks in Greenhouse Technology and Overview for Smart Agriculture Development. *Applied Sciences*. 10(11), Art. ID 3835. https://doi.org/10.3390/app10113835.

Gao, Y., Song, X., Liu, C. et al. (2014) Feedback Feed-forward Linearization and Decoupling for Greenhouse Environment Control. In: *2014 International Conference on Mechatronics and Control (ICMC), 3-5 July 2014*, *Jinzhou, China*. New York, USA, IEEE. pp. 179-183.

Gurban, E. H., Dragomir, T. L. & Andreescu, G.-D. (2014) Greenhouse Climate Control Enhancement by Using Genetic Algorithms. *Journal of Control Engineering and Applied Informatics*. 16(3), 35-45.

Lakomy, K. & Madonski, R. (2021) Cascade Extended State Observer for Active Disturbance Rejection Control Applications under Measurement Noise. *ISA Transactions*. 109, 1-10. https://doi.org/10.1016/j.isatra.2020.09.007.

Lammari, K., Bounaama, F., Ouradj, B. et al. (2020) Constrained GA PI sliding mode control of indoor climate coupled MIMO greenhouse model. *Journal of Thermal Engineering*. 6(3), 313-326. https://doi.org/10.18186/thermique.711554.

Li, S., Yang, J., Chen, W.-H. et al. (2012) Generalized Extended State Observer Based Control for Systems With Mismatched Uncertainties. *IEEE Transactions on Industrial Electronics*. 59(12), 4792–4802. https://doi.org/10.1109/tie.2011.2182011.

Luan, X., Shi, Y. & Liu, F. (2012) Unscented Kalman filtering for greenhouse climate control systems with missing measurement. *International Journal of Innovative Computing Information and Control*. 8(3), 2173-2180.

Madonski, R. & Herman, P. (2015) Survey on methods of increasing the efficiency of extended state disturbance observers. *ISA Transactions*. 56, 18-27. https://doi.org/10.1016/j.isatra.2014.11.008.

Nicholas, A. & Maria, A. (2013) Kalman Filter Riccati Equation for the Prediction, Estimation, and Smoothing Error Covariance Matrices. *Mathematical Problems in Engineering*. 2013, Art. ID 249594. https://doi.org/10.1155/2013/249594.

Qi, G., Li, X. & Chen, Z. (2021) Problems of Extended State Observer and Proposal of Compensation Function Observer for Unknown Model and Application in UAV. *IEEE Transactions on Systems, Man, and Cybernetics: Systems*. 52(5), 2899-2910. https://doi.org/10.1109/tsmc.2021.3054790.

Schneider, R. & Georgakis, C. (2013) How To NOT Make the Extended Kalman Filter Fail. *Industrial and Engineering Chemistry Research*. 52(9), 3354–3362. https://doi.org/10.1021/ie300415d.

Shao, S. & Gao, Z. (2016) On the Conditions of Exponential Stability in Active Disturbance Rejection Control based on Singular Perturbation Analysis. *International Journal of Control*. 90(10), 2085-2097. https://doi.org/10.1080/00207179.2016.1236217.

Sun, H., Madonski, R., Li, S. et al. (2021) Composite Control Design for Systems With Uncertainties and Noise Using Combined Extended State Observer and Kalman Filter. *IEEE Transactions on Industrial Electronics*. 69(4), 4119-4128. https://doi.org/10.1109/TIE.2021.3075838.

Wang, L., Zhang, Y., Xu, M. et al. (2024) Predictive control for greenhouse temperature and humidity and energy optimization by improved NMPC objective function algorithm. *International Journal of Agricultural & Biological Engineering*. 17(5), 128–136. https://doi.org/10.25165/j.ijabe.20241705.8241.

Wu, M., Xiao, H., Lu, C. et al. (2024) Research on decoupling greenhouse temperature and humidity based on feedback linearization. *Journal of Electrical Systems*. 20(2), 394-399. https://doi.org/10.52783/jes.1192.

Xiong, S., Wang, W., Liu, X. et al. (2015) A novel extended state observer. *ISA Transactions.* 58, 309–317. https://doi.org/10.1016/j.isatra.2015.07.

Xue, W. & Huang, Y. (2015) Performance analysis of active disturbance rejection tracking control for a class of uncertain LTI systems. *ISA Transactions*. 58, 133-154. https://doi.org/10.1016/j.isatra.2015.05.001.

Xue, W. & Huang, Y. (2018) Performance analysis of 2-DOF tracking control for a class of nonlinear uncertain systems with discontinuous disturbances. *International Journal of Robust and Nonlinear Control*. 28(4), 1456-1473. https://doi.org/10.1002/rnc.3972.

Zhang, S., Guo, Y., Zhao, H. et al. (2020) Methodologies of control strategies for improving energy efficiency in agricultural greenhouses. *Journal of Cleaner Production.* Art. ID 122695. https://doi.org/10.1016/j.jclepro.2020.122695.

Zhang, Y., Shen, Y., Liu, H. et al. (2025) A composite sliding mode controller with extended disturbance observer for 4WSS agricultural robots in unstructured farmlands. *Computers and Electronics in Agriculture*. 232, art. ID 110069. https://doi.org/10.1016/j.compag.2025.110069.